2015 CHATS on Applied Superconductivity Workshop

Numerical Simulation on Magnetic Field generated by Screening Current in REBCO coils

Hiroshi UEDA(Osaka University)

So NOGUCHI (Hokkaido University)

Ayako MATSUMI, Ayumu MOCHIDA, Yohei IMAICHI (Waseda University)

Atsushi ISHIYAMA (Waseda University)

This research was supported Grant-in-Aid for Scientific Research (C), the Ministry of Education, Science, Sports and Culture (No.25420253).

Contents

- Background
- Numerical method for screening current in REBCO tape
- Developed numerical simulation
- Experiment
- Example of experimental and numerical results
- Conclusion

Contents

Current distribution in REBCO tape

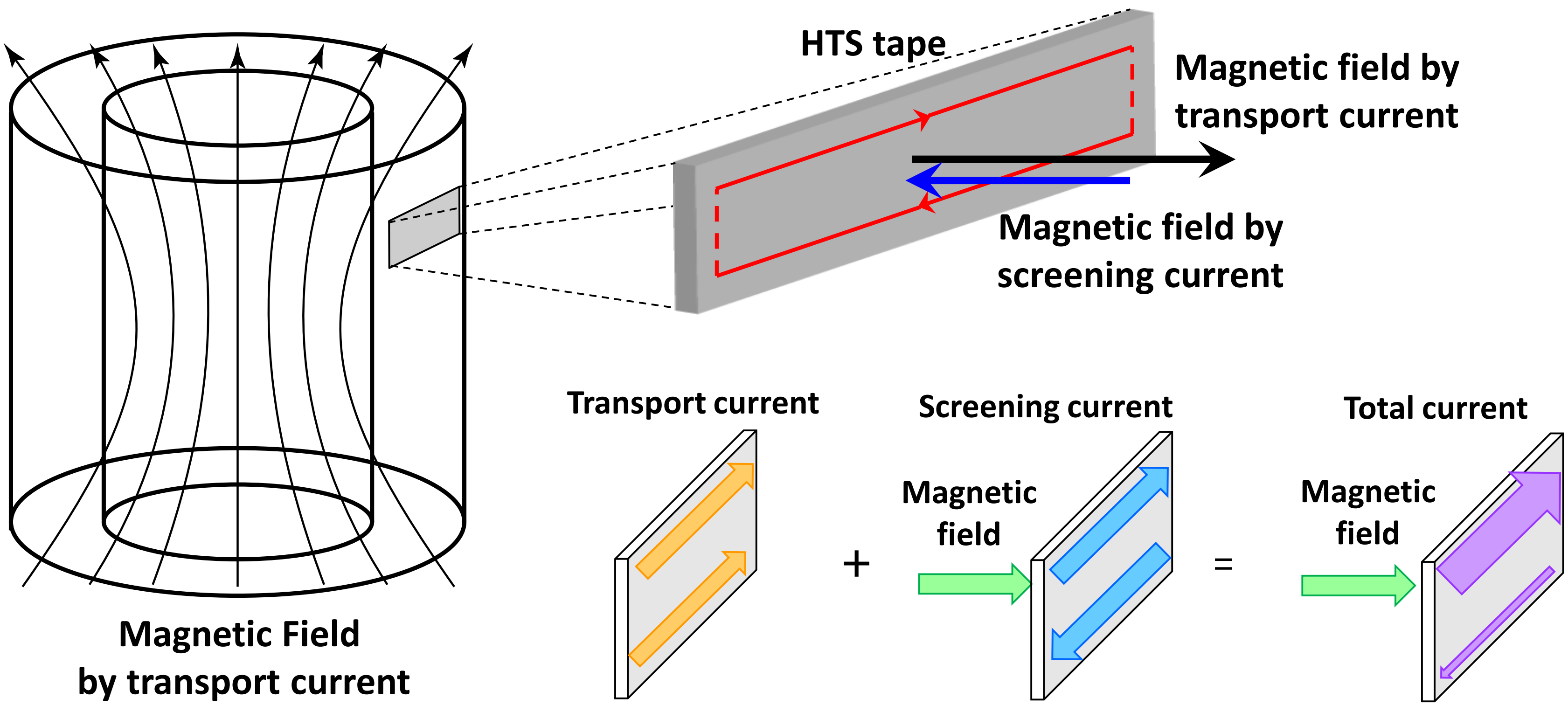

- Diffusion of field
- Flux creep

Screening current

(1) Field reduction

Screening-current field generates in the opposite direction of the field by the transport current, thus reducing the magnetic field.

(2) Accuracy of field distribution

Screening current leads to non-uniform current distributions in the HTS tape, and the field quality is deteriorated.

(3) Temporal stability

Screening-current field is time-dependent, thus affecting the time stability of the magnetic field.

(4) Field repeatability

Screening current remains in HTS tape after the repetition of charging and discharging, thus not repeatable the magnetic field distribution.

Prediction and reduction of screening-current field

We developed a novel numerical simulation.

Contents

Choice of model and formulation

Model and formulation		Choice
Model of coil winding (Pancake winding, Layer winding)		✓ Assembly of 1 turn coil
		✓ Consideration of winding configuration
Model of superconducting property	E-J characteristics	✓ n-value model
		✓ Flux flow and creep model
		✓ Percolation model
	Distribution of property in tape (local Ic variation)	✓ Uniform
		✓ Non-uniform
Formulation	Model of tape	✓ Thin-approximation (neglect of 'thickness' effect)
		✓ 'thickness' effect
	Technique	✓ T method
		✓ A method
	Magnetic coupling among tapes	✓ No coupling -> External field
		✓ Far: no coupling, Neighborhood: coupling
		✓ All interactions are considered

Coil winding

- ✓ Assembly of 1 turn coil
  (the closed path of screening current in each 1 turn coil)
- ✓ Pancake winding, Layer winding
  (the end-to-end path of screening current in winding tape)

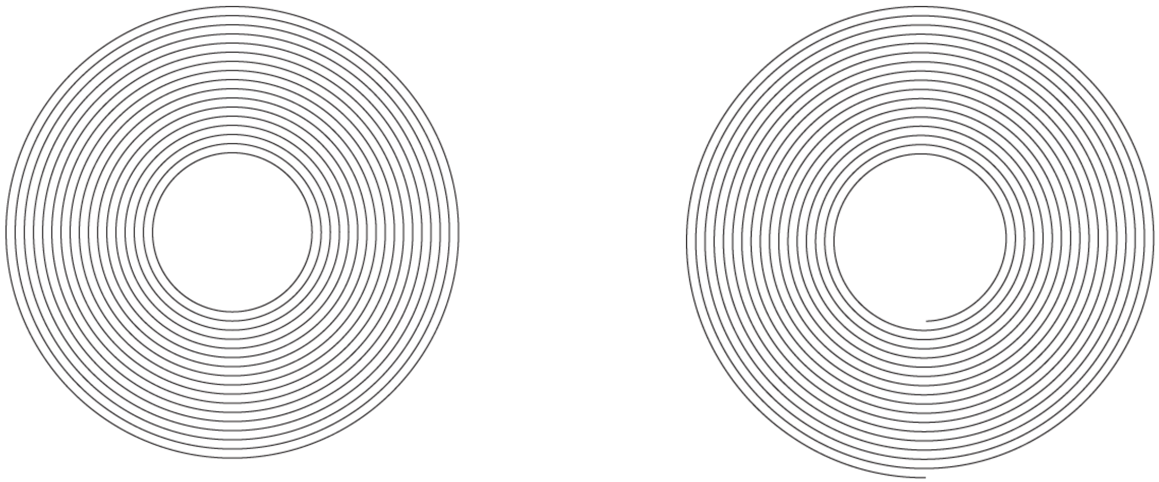

Superconducting characteristics

Critical state model

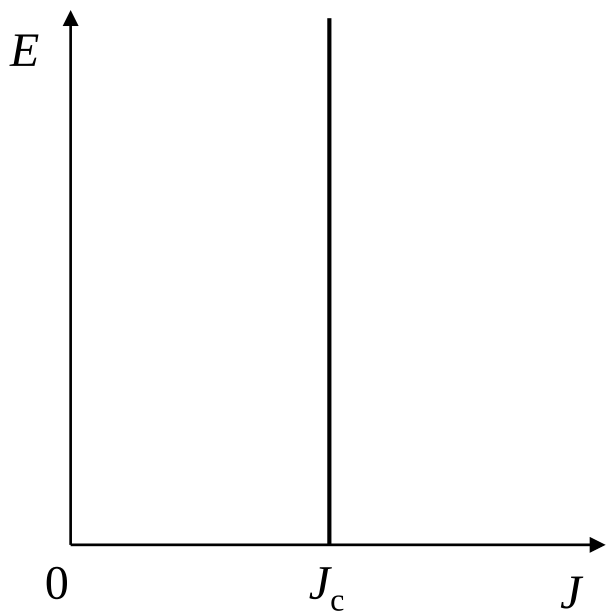

n-value model

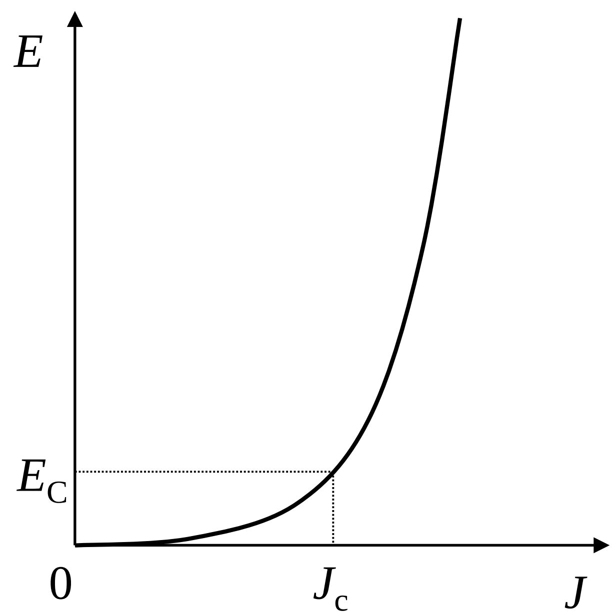

$$\boldsymbol{J} = J_c(|\boldsymbol{B}|)\frac{\boldsymbol{E}}{|\boldsymbol{E}|} \quad \text{if } |\boldsymbol{E}| \neq 0 \;\Rightarrow\; J = J_c$$

$$\frac{\partial \boldsymbol{J}}{\partial t} = 0 \quad \text{if } |\boldsymbol{E}| = 0$$

$$E = E_c\left(\frac{J}{J_c}\right)^n$$

Superconducting characteristics

n-value model

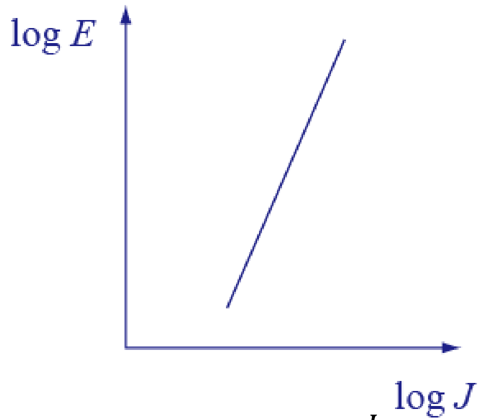

Percolation model

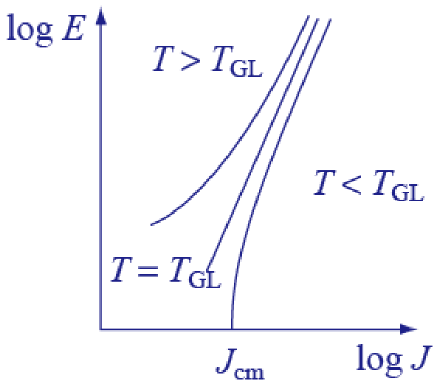

$$
\begin{aligned}
E(J) &= \rho_{ff} \int_0^J Q(J)\,dJ \\
&= \frac{\rho_{ff}}{m+1} J \left(\frac{J}{J_0(T,B)}\right)^m \left(1 - \frac{J_{\mathrm{cm}}(T,B)}{J}\right)^{m+1} && T < T_{\mathrm{GL}} \\
&= \frac{\rho_{ff}}{m+1} J \left(\frac{J}{J_0(T,B)}\right)^m && T = T_{\mathrm{GL}} \\
&= \frac{\rho_{ff}}{m+1} |J_{\mathrm{cm}}(T,B)| \left(\frac{|J_{\mathrm{cm}}(T,B)|}{J_0(T,B)}\right)^m \left\{\left(1 + \frac{J}{|J_{\mathrm{cm}}(T,B)|}\right)^{m+1} - 1\right\} && T > T_{\mathrm{GL}}
\end{aligned}
$$

K. Yamafuji and T. Kiss: “Current-voltage characteristics near the glass-liquid transition in high-Tc superconductors”, Physica C **290** (1997) 9-22

Formulation

- ✓ FEM or BEM (Maxwell equation, Ohm's law, Biot-Savart law...)
- ✓ Magnetic coupling among tapes
  - ✓ Biot-Savart law on an assumption of uniform current except for target element
  - ✓ Unknown current distribution for all element
- ✓ Thin-film approximation

  The current direction is assumed to be parallel to the wide face of the tape.

Thin-film approximation

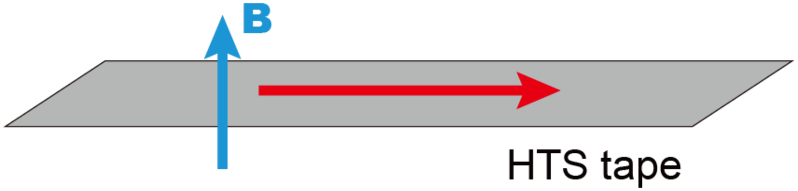

'thickness' effect

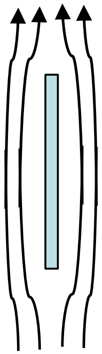

Numerical method for screening current

	Axisymmetric		3D -> 2D	3D
	Y. Yanagisawa[(1)(2)]	N. Amemiya[(3)]	S. Noguchi[(4)]	H. Ueda[(5)(6)]
	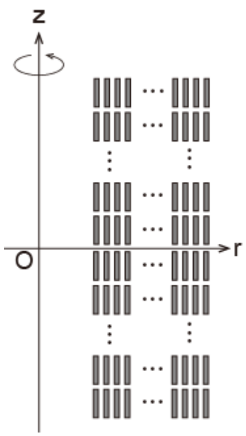		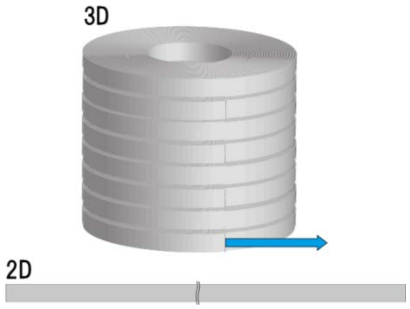	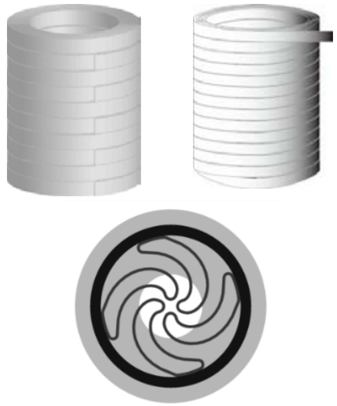
Analysis objects	✓ Circular coil ✓ No difference between Pancake winding and Layer winding		✓ Circular and non-circular coil ✓ Difference between Pancake winding and Layer winding	
Coupling among tapes	**No** Magnetic field by uniform current (Complete elliptic integral)	**Partially Yes** ✓ Neighborhood: Yes ✓ Far: No (Uniform current)	**No** Magnetic field by uniform current (Biot-Savart law)	**Yes** ✓ Neighborhood: Yes ✓ Far: Multipole expansion (considered in iteration solver)

(1) Y. Yanagisawa, et at., Physica C, 469 (2009) 1996–1999.
(2) Y. Yanagisawa, et al., IEEE Trans. Appl. Supercond., 20 (2010) 744-747.
(3) N. Amemiya, et al., Supercond. Sci. Technol, 21 (2008) 095001.
(4) R. Itoh, et al., IEEE Trans. Appl. Supercond., 23 (2013) 4600905.
(5) H. Ueda, et al., IEEE Trans. Appl. Supercond., 23 (2013) 4100805.
(6) H. Ueda, et al., IEEE Trans. Appl. Supercond., 24 (2014) 4701505.

Contents

- Background
- Numerical method for screening current in REBCO tape
- **Developed numerical simulation**
- Experiment
- Example of experimental and numerical results
- Conclusion

Analysis objects

- ✓ **MRI:** Non-axisymmetric field distribution by gradient coil

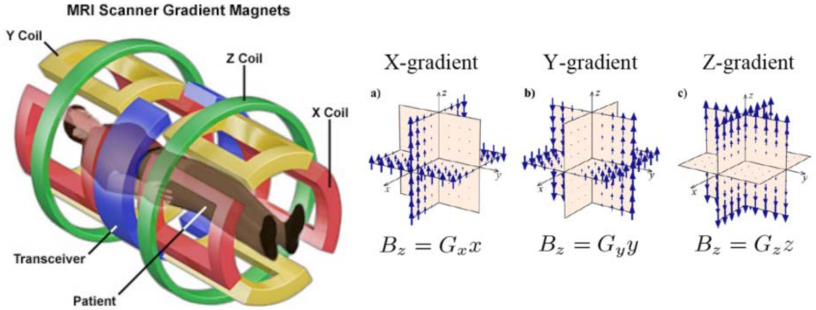

http://www.magnet.fsu.edu/education/tutorials/magnetacademy/mri/fullarticle.html

- ✓ **Cyclotron:** Non-circular coil

- ✓ **Pancake winding, Layer winding**

Path of screening current in tape
Time constant

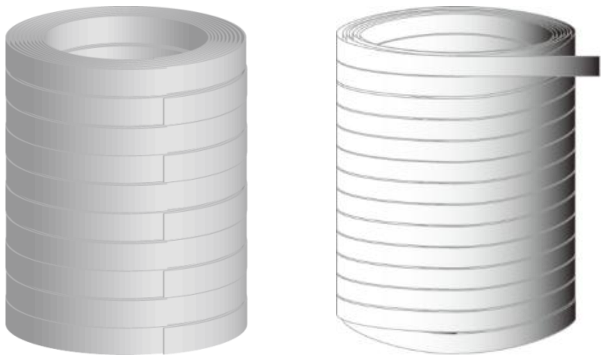

Formulation of 3-dimensinonal magnetic analysis

Formulation

Analysis model： 3D-FEM including Integral term
Thin-film approximation
Able to consider a difference between Layer winding and Pancake winding

$$\boldsymbol{\nabla} \times (\rho \boldsymbol{\nabla} \times \boldsymbol{T}) = -\frac{\partial \boldsymbol{B}}{\partial t}$$

$$\boldsymbol{\nabla} \times \boldsymbol{T} = \boldsymbol{J}$$

$$\boldsymbol{B} = \boldsymbol{B_e} + \boldsymbol{B}_0$$

$$\boldsymbol{B}_e = \frac{\mu_0}{4\pi} \int_V \frac{\boldsymbol{J}' \times \boldsymbol{R}}{R^3} dV'$$

$\boldsymbol{J}$: Current density in tape
$\boldsymbol{E}$: Electric field
ρ: Resistivity
$\boldsymbol{B}_e$: Magnetic field by current in tape
$\boldsymbol{B}_0$: External magnetic field
$\boldsymbol{R}$: Vector from source point, $\boldsymbol{r}'$ to observed point, $\boldsymbol{r}$

$$\boldsymbol{\nabla} \times \rho(\boldsymbol{\nabla} \times \boldsymbol{T}) + \frac{\mu_0}{4\pi}\frac{\partial}{\partial t}\int_V \frac{(\boldsymbol{\nabla} \times \boldsymbol{T}') \times \boldsymbol{R}}{R^3} dV' = -\frac{\partial \boldsymbol{B}_0}{\partial t}$$

Thin-film approximation $\boldsymbol{T} = T\boldsymbol{n}$ $\boldsymbol{T}' = T'\boldsymbol{n}$

d ：thickenss of superconductor

$$\{\boldsymbol{\nabla} \times \rho(\boldsymbol{\nabla}T \times \boldsymbol{n})\} \cdot \boldsymbol{n} + \frac{\mu_0 d}{4\pi}\frac{\partial}{\partial t}\int_S \frac{(\boldsymbol{\nabla}T' \times \boldsymbol{n}') \times \boldsymbol{R}}{R^3} \cdot \boldsymbol{n} dS' = -\frac{\partial \boldsymbol{B}_0}{\partial t} \cdot \boldsymbol{n}$$

Numerical technique

$$\{\boldsymbol{\nabla} \times \rho(\boldsymbol{\nabla} T \times \boldsymbol{n})\} \cdot \boldsymbol{n} + \frac{\mu_0 d}{4\pi} \frac{\partial}{\partial t} \int_S \frac{(\boldsymbol{\nabla} T' \times \boldsymbol{n}') \times \boldsymbol{R}}{R^3} \cdot \boldsymbol{n} \, dS' = -\frac{\partial \boldsymbol{B}_0}{\partial t} \cdot \boldsymbol{n}$$

FEM

Integral term

Superconducting property

$$E = E_c \left(\frac{J}{J_c(B, \theta, T)} \right)^{n(B,\theta,T)}$$

⇩

$$\rho = \frac{E_c}{J_c(B, \theta, T)} \left(\frac{J}{J_c(B, \theta, T)} \right)^{n(B,\theta,T)-1}$$

Strong nonlinearity

Modified Newton-Raphson method accelerated by using a Line Search

K. Fujiwara et al. “The Newton–Raphson Method Accelerated by Using a Line Search —Comparison Between Energy Functional and Residual Minimization”, pp.1724-1727, IEEE Trans. on Magn, vol.41, 2005

Numerical method feature

FEM

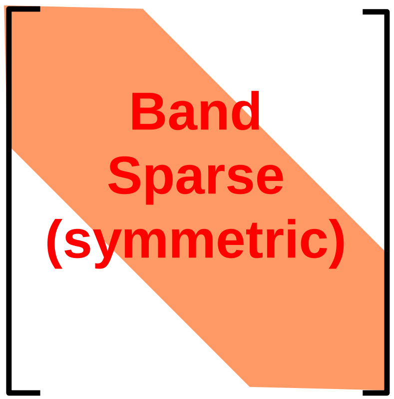

- On a set of partial differential equations
- Discretization in the domain
- Sparse and large systems
- Boundary conditions are approximated in infinity
- Nonlinear material can be treated

BEM or Integral term

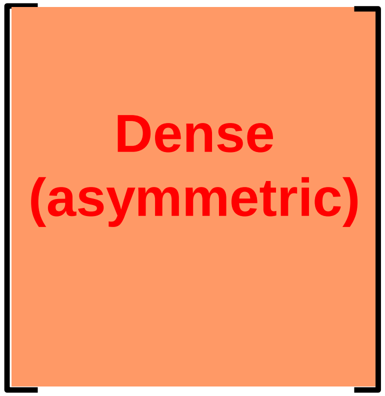

- On integral equations
- Discretization on the surface
- Dense and smaller systems
- Boundary conditions are automatically satisfied in infinity
- Linear material can be treated with accuracy

Numerical technique

$$\{\boldsymbol{\nabla} \times \rho(\boldsymbol{\nabla} T \times \boldsymbol{n})\} \cdot \boldsymbol{n} + \frac{\mu_0 d}{4\pi} \frac{\partial}{\partial t} \int_S \frac{(\boldsymbol{\nabla} T' \times \boldsymbol{n}') \times \boldsymbol{R}}{R^3} \cdot \boldsymbol{n}\, dS' = -\frac{\partial \boldsymbol{B}_0}{\partial t} \cdot \boldsymbol{n}$$

FEM

Integral term

Superconducting property

$$E = E_c \left(\frac{J}{J_c(B, \theta, T)} \right)^{n(B,\theta,T)}$$

$$\rho = \frac{E_c}{J_c(B, \theta, T)} \left(\frac{J}{J_c(B, \theta, T)} \right)^{n(B,\theta,T)-1}$$

Strong nonlinearity

A process of the computation of all pairwise interactions among sources is needed similar to the boundary element method.

Fast Multipole Method + Iterative Solver (GMRES)

Modified Newton-Raphson method accelerated by using a Line Search

K. Fujiwara et al. "The Newton–Raphson Method Accelerated by Using a Line Search —Comparison Between Energy Functional and Residual Minimization", pp.1724-1727, IEEE Trans. on Magn, vol.41, 2005

Fast multipole method:FMM

Conventional method

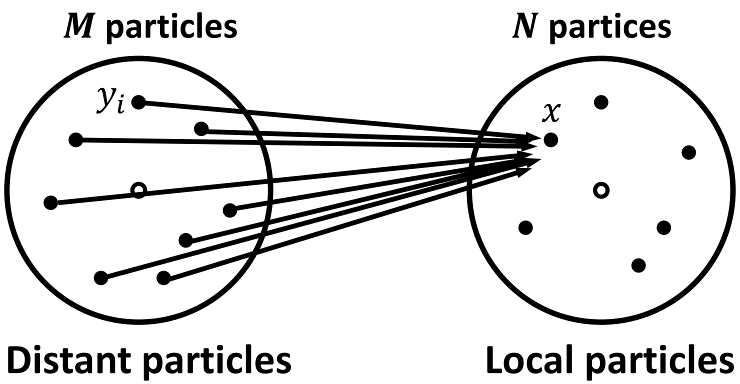

$$\Phi(x) = \sum_{i=1}^{M} \frac{q_i}{|\overrightarrow{y_i x}|}$$

- ✓ The FMM were developed for the fast evaluation of potential fields generated by large number of sources (e.g. the gravitational and electrostatic potential fields governed by Laplace equation) as it is called the *N*-body problem.
- ✓ The *N*-body problem in numerical simulations describes the computation of all pairwise interactions among *N* bodies with $O(N^2)$ runtime complexity.

Fast multipole method:FMM

Multipole/Local expansion

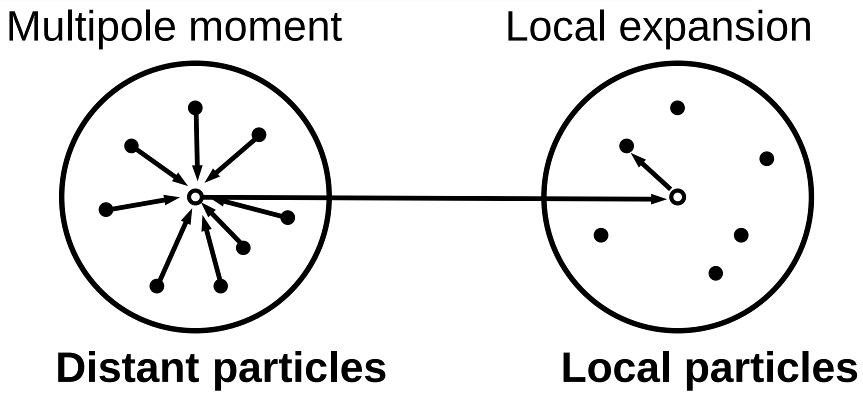

Multipole expansion allows one to group sources that lie close together and treat them as if they are a single source.

- ✓ Multipole moments represent distant particle groups.
- ✓ The multipole moment associated with a distant group can be translated into the coefficient of the local expansion associated with a local group.
- ✓ Local expansion is introduced to evaluate the contribution from distant particles in the form of a series.

L. Greengard and V. Rokhlin: “A new version of the fast multipole method for the Laplace equation in three dimensions,” *Acta Numerica*, vol. 6, pp. 229-269, Jan.1997.

Procedure of FMM

$$\boldsymbol{L}_{n,m}(x_0) = \sum_{n'=0}^{\infty} \sum_{m'=-n'}^{n'} (-1)^n \overline{S_{n+n',m+m'}(\overrightarrow{Ox_0})} \boldsymbol{M}_{n',m'}(O)$$

$$\boldsymbol{M}_{n,m}(O) = \int_{S_k} (\nabla T' \times \boldsymbol{n}') \times R_{n,m}(\overrightarrow{OQ})\, dS_k$$

$$\boldsymbol{M}_{n,m}(O') = \sum_{n'=0}^{\infty} \sum_{m'=-n'}^{n'} R_{n',m'}(\overrightarrow{O'O}) \boldsymbol{M}_{n-n',m-m'}(O')$$

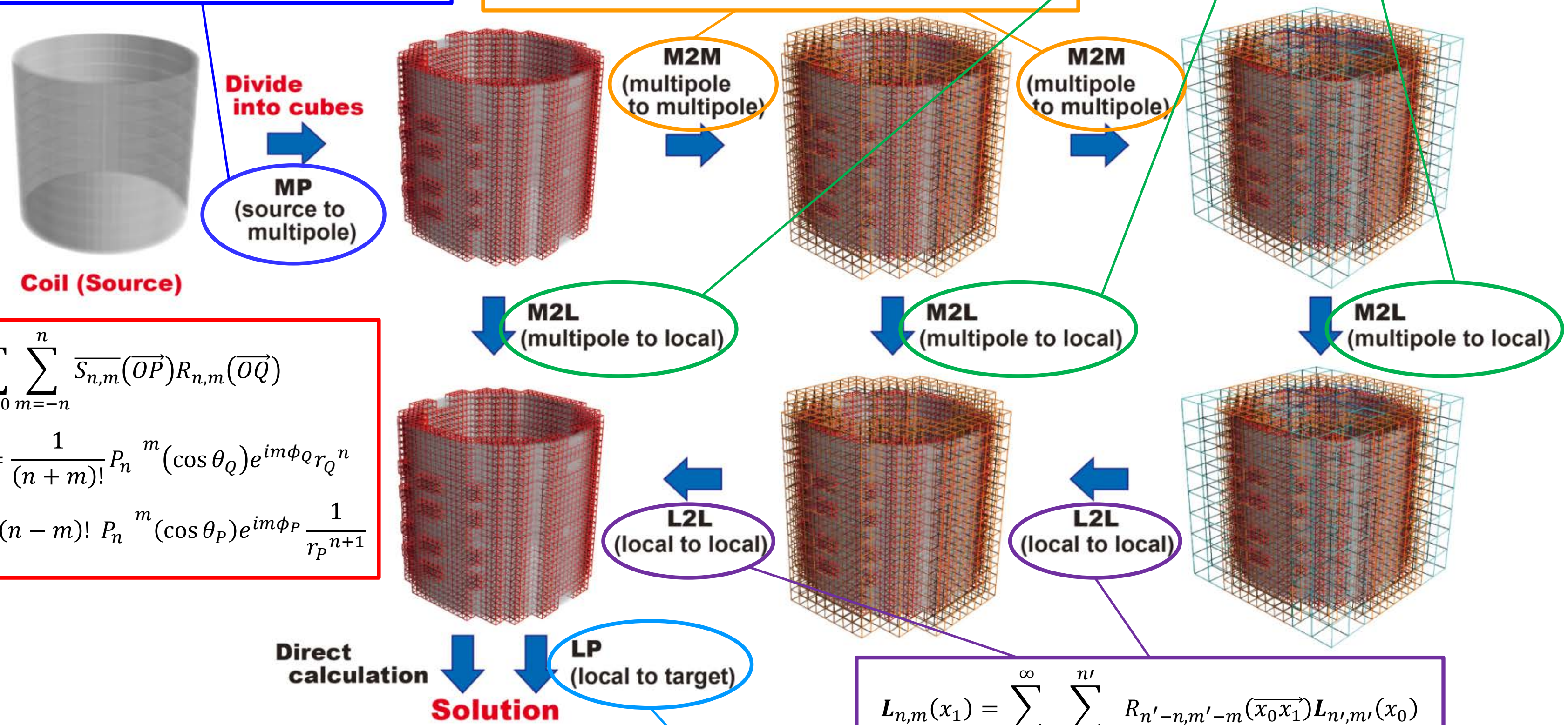

$$\frac{1}{R} = \frac{1}{|\overrightarrow{QP}|} = \sum_{n=0}^{\infty} \sum_{m=-n}^{n} \overline{S_{n,m}(\overrightarrow{OP})} R_{n,m}(\overrightarrow{OQ})$$

$$R_{n,m}(\overrightarrow{OQ}) = \frac{1}{(n+m)!} P_n{}^m(\cos\theta_Q) e^{im\phi_Q} r_Q{}^n$$

$$S_{n,m}(\overrightarrow{OP}) = (n-m)!\ P_n{}^m(\cos\theta_P) e^{im\phi_P} \frac{1}{r_P{}^{n+1}}$$

$$\boldsymbol{L}_{n,m}(x_1) = \sum_{n'=0}^{\infty} \sum_{m'=-n'}^{n'} R_{n'-n,m'-m}(\overrightarrow{x_0x_1}) \boldsymbol{L}_{n',m'}(x_0)$$

$$\boldsymbol{H}(x) = \sum_{n=0}^{\infty} \sum_{m=-n}^{n} R_{n,m}(\overrightarrow{x_0x}) \boldsymbol{L}_{n,m}(x_0)$$

Accuracy of the method

Parameter of FMM influenced calculation accuracy

- ✓ Mesh of finite element
- ✓ Order of Gauss-Legendre quadrature
- ✓ Determination of far or neighborhood in FMM

  Far: FMM Neighborhood: Direct calculation
- ✓ Order of multipole/local expansion
- ✓ Tolerance of nonlinear calculation for superconductor

Accuracy (field-homogeneity)

Inner diameter (mm)	50
Outer diameter (mm)	158.5
Number of turns／single pancake	280
Number of single pancake	30
Gap between single pancakes (mm)	0.8
Transport current (A)	200

Legendre expansion and homogeneity on DSV of $\rho = 12.5\ \mathrm{mm}$

	Biot-Savart law		FMM	
order, n	Field, b_n (T)	homogeneity (ppm)	Field, b_n (T)	homogeneity (ppm)
0	10.374		10.375	
2	-5.72×10^{-2}	-5.51×10^{3}	-5.71×10^{-2}	-5.51×10^{3}
4	-7.28×10^{-4}	-7.01×10	-7.28×10^{-4}	-7.02×10
6	-4.64×10^{-6}	-4.48×10^{-1}	-4.64×10^{-6}	-4.47×10^{-1}
8	-2.34×10^{-8}	-2.25×10^{-3}	-2.31×10^{-8}	-2.23×10^{-3}
10	5.72×10^{-8}	5.08×10^{-3}	5.62×10^{-8}	5.42×10^{-3}
12	-5.30×10^{-8}	-5.10×10^{-3}	-5.32×10^{-8}	-5.13×10^{-3}
14	4.49×10^{-8}	4.33×10^{-3}	4.88×10^{-8}	4.71×10^{-3}
16	-2.34×10^{-8}	-2.26×10^{-3}	-2.52×10^{-8}	-2.43×10^{-3}
18	1.92×10^{-8}	1.85×10^{-3}	2.28×10^{-8}	2.20×10^{-3}
20	-1.85×10^{-8}	-1.78×10^{-3}	-2.03×10^{-8}	-1.96×10^{-3}
Total		-5.58×10^{3}		-5.58×10^{3}

Contents

- Background
- Numerical method for screening current in REBCO tape
- Developed numerical simulation
- Experiment
- Example of experimental and numerical results
- Conclusion

Measurement setup

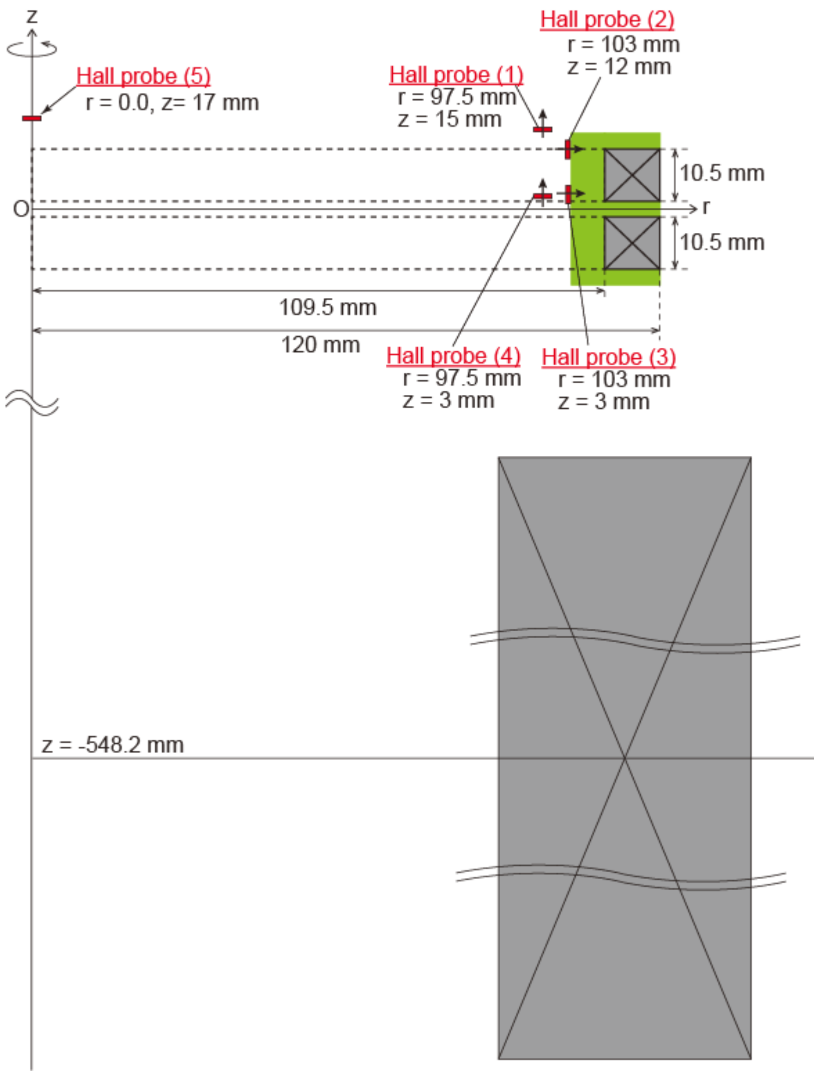

REBCO coil

LTS magnet
for generating external field

JMTD-10T100E1
Bore diameter: 100 mm
Maximum field at center: 10 T
Uniformity: 0.088 %

2T −z direction

Current patterns

(1) Alternate triangular wave
  (a) Self-field of HTS coil
  (b) External field and then self-field

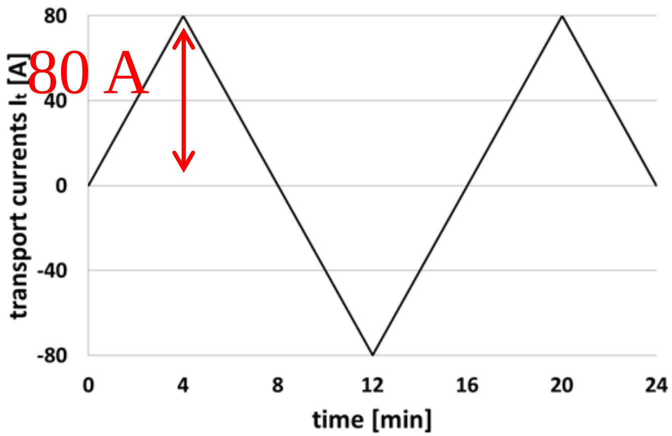

(2) Charge and hold
  (a) Self-field of HTS coil

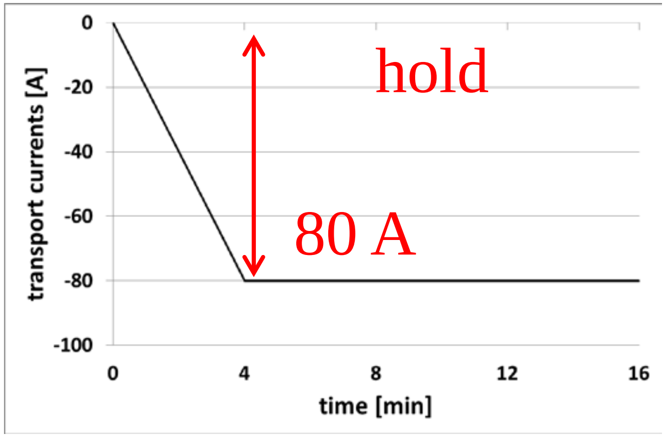

*sweep rate: 20 A/min
External field is applied by LTS magnet.

Contents

- Background
- Numerical method for screening current in REBCO tape
- Developed numerical simulation
- Experiment
- Example of experimental and numerical results
- Conclusion

Results

<Ex. (1)-(a) Alternate self-field >

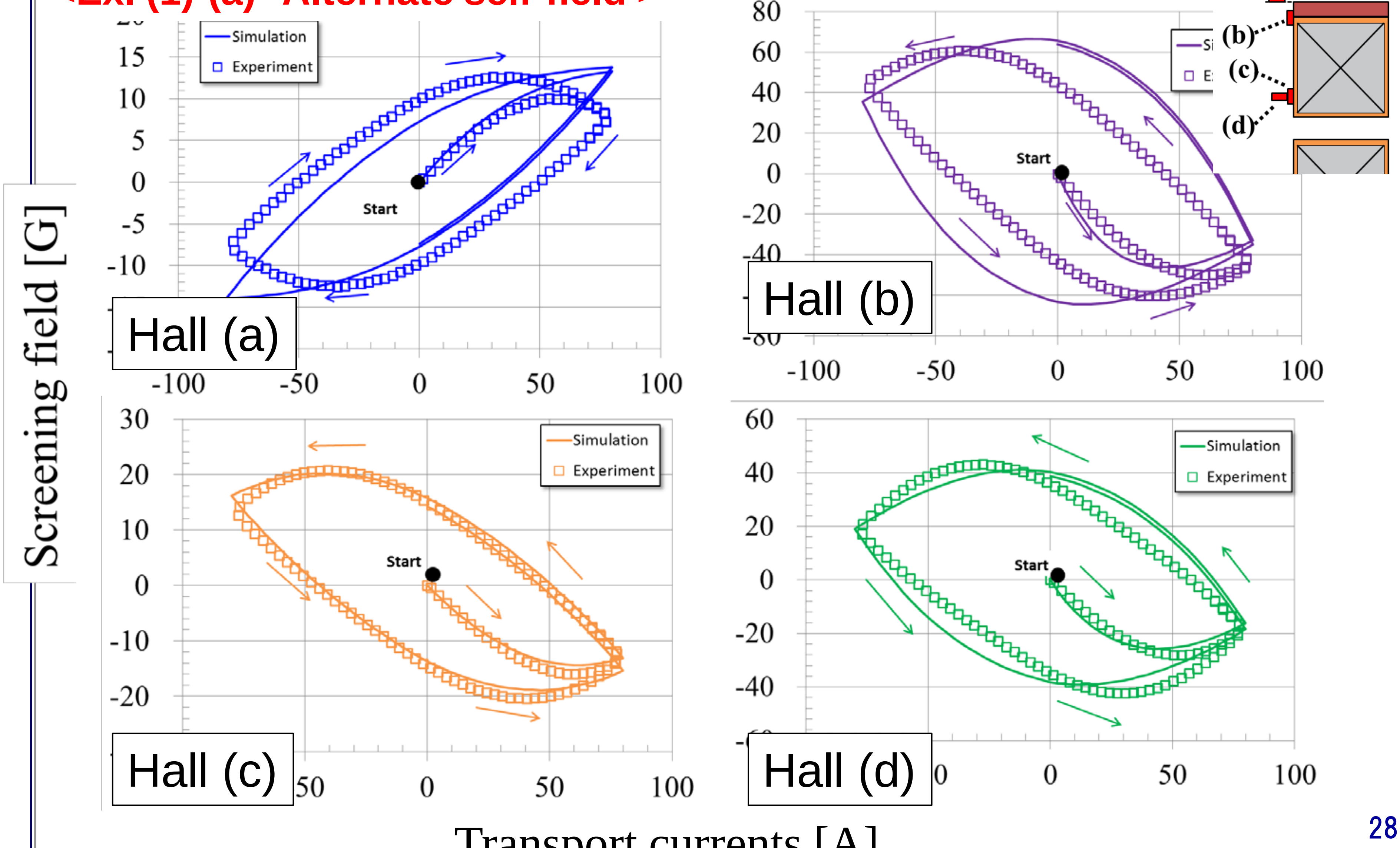

Results

<Ex. (1)-(b) External field and then alternate self-field >

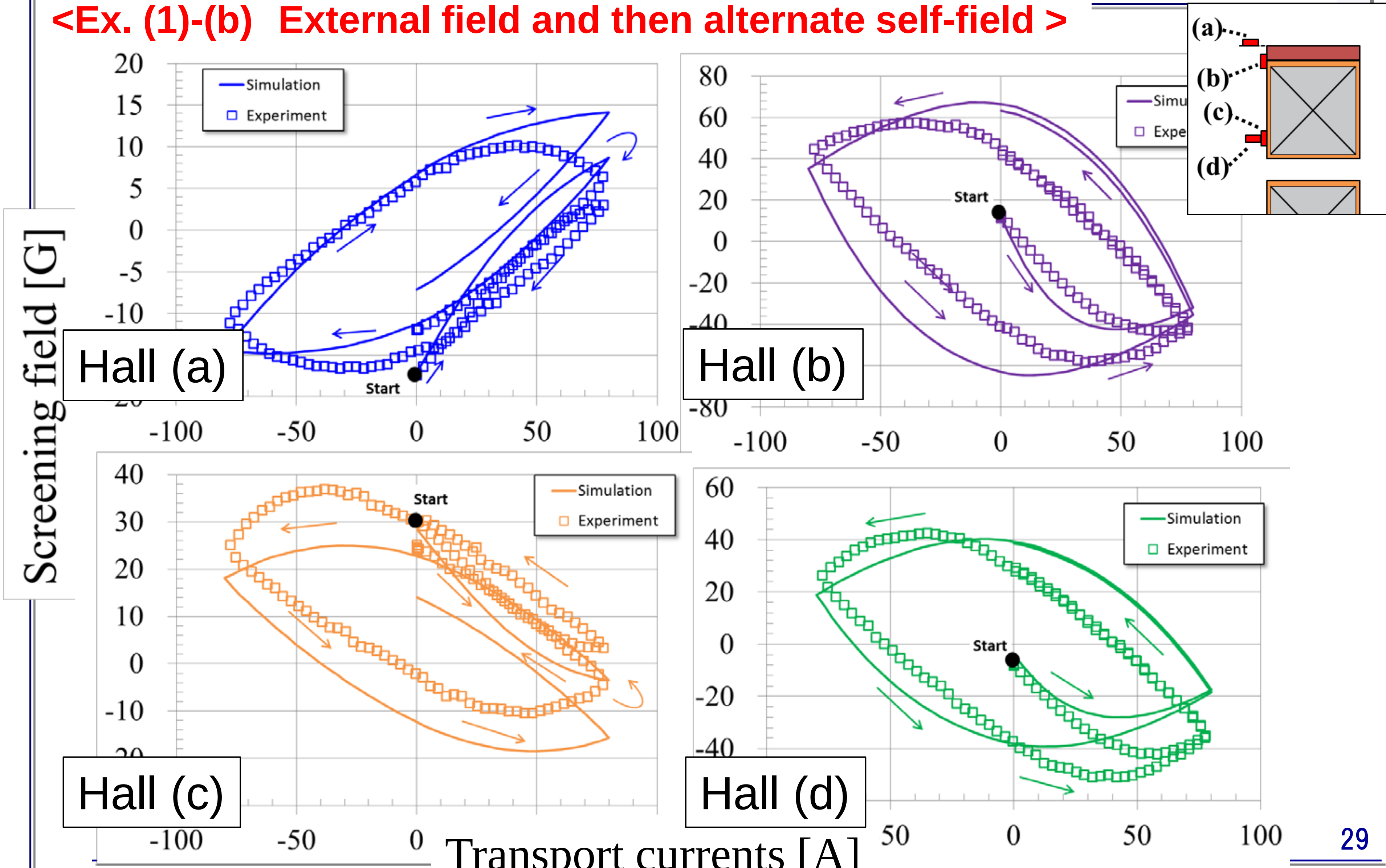

Charge and hold

<Ex. (2) Charge and hold self-field>

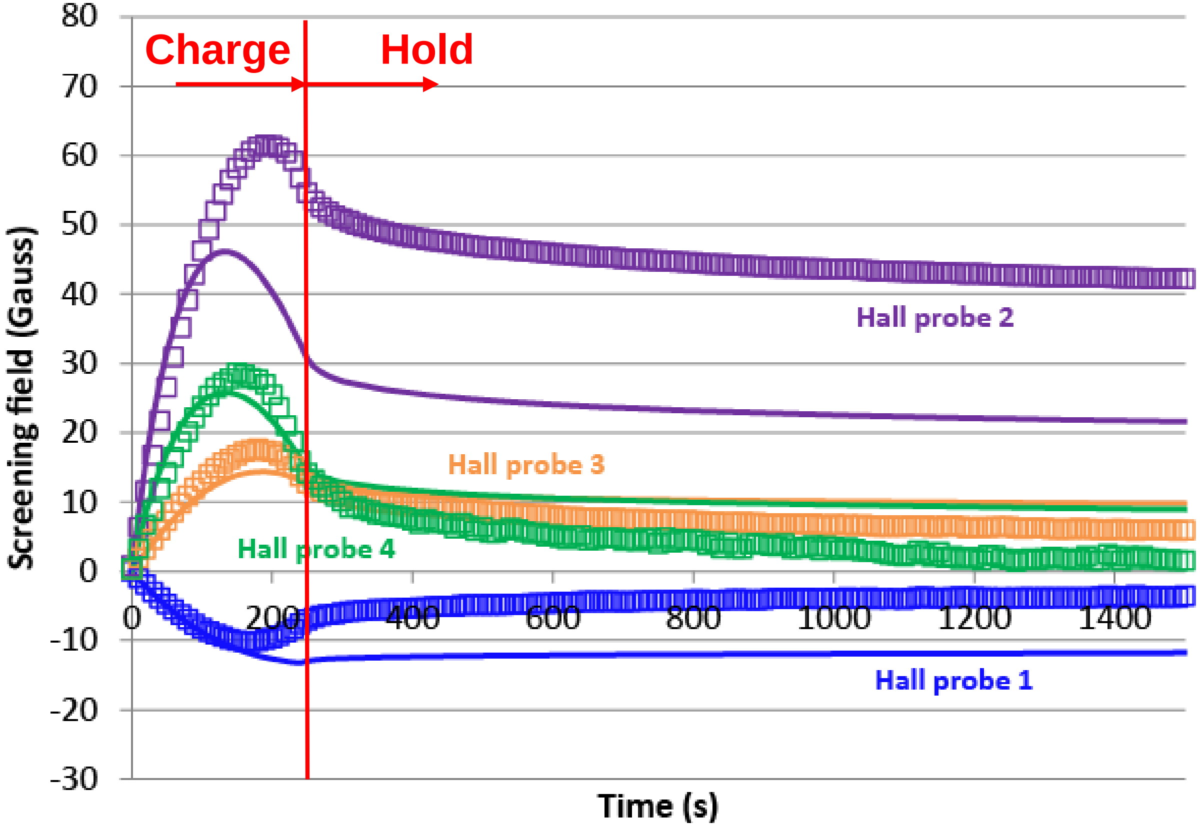

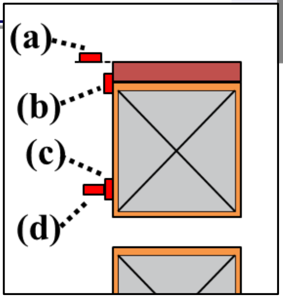

Difference

The differences between the experimental and numerical results are assumed to be due to

- ✓ Measuring limit of a coil constant
- ✓ Location accuracy of Hall probe
- ✓ Difference of superconducting characteristic between the short sample and the used in coil winding.

Contents

- Background
- Numerical method for screening current in REBCO tape
- Developed numerical simulation
- Experiment
- Example of experimental and numerical results
- Conclusion

Conclusion

- ✓ We investigated the current distribution in the HTS tape and the spatial and temporal behavior of the magnetic field using our developed three-dimensional numerical simulation.
- ✓ The numerical results agree well with the experimental results. Additionally, we confirmed the validity of the numerical simulation.
- ✓ We intend to utilize the developed simulation code to suppress the screening current and to investigate the influence of the I_c distribution on the REBCO tape.
- ✓ These data are essential for the development and design of NMRs, MRIs, and accelerators, which require high accuracy and temporally stable magnetic field.

In future

✓ We evaluated the following issues using a developed simulation code.

◆ 10T-class small bore REBCO coil

coil construction and screening-current field measurement

◆ 10T-class human whole-body REBCO-MRI

coil design and homogeneity prediction

◆ Air-core cyclotron using REBCO coil

coil design and field-distribution prediction

These results will be reported in future, MT-24 and ASC 2016.

Thank you for your attention.